Bulletin of Electrical Engineering and Informatics
Vol. 15, No. 3, June 2026, pp. 2030~2044
ISSN: 2302-9285, DOI: 10.11591/eei.v15i3.11199

Enhancing solar power generation efficiency through chaotic beetle swarm optimization for constant power generation

Sreenivasan Ramachandran, Ramkumar Ravindran
Department of Electrical and Electronics Engineering, School of Engineering and Technology, Dhanalakshmi Srinivasan University, Samayapuram, India

Article Info

Article history:

Received Aug 13, 2025
Revised Mar 13, 2026
Accepted Apr 19, 2026

Keywords:

Chaotic beetle swarm optimization algorithm
Dual stage XBoost converter
Photovoltaic system
RBFNN-MPPT
Renewable energy source

ABSTRACT

The necessity for more and cleaner sustainable energy sources to generate power is increasing because of the reduction of fossil fuel supplies and their negative impacts on the environment. This research addresses the requiring crucial for optimized solar power systems in the weather change issues. In the beginning, the photovoltaic (PV) system's voltage is enhanced by dual stage XBoost converter (DSXBC) with little voltage stress and maximum voltage gain. Also, the radial bias function neural network (RBFNN)-maximum power point tracking (MPPT) tracks the PV system's uppermost power and its parameters are fine-tuned by chaotic beetle swarm optimization (CBSO) algorithm. By integrating chaotic dynamics within the optimization process, CBSO runs a robust and efficient approach to navigating the complex search space related with MPPT. The MATLAB tool is utilized to reveal the efficacy of developed approach for allowing constant power generation in solar power generation systems with efficacy of 99.74% and tracking efficiency of 98.9% in steady state condition, thereby enabling continuous power generation.

Corresponding Author:

Sreenivasan Ramachandran
Department of Electrical and Electronics Engineering, School of Engineering and Technology
Dhanalakshmi Srinivasan University
Samayapuram, Trichy, Tamilnadu, India
Email: srini.vasan256@gmail.com

1. INTRODUCTION

Because of the rising request for energy, the fossil fuels are exploited more rapidly as the main reason of power production [1]. Therefore, the attention is transformed from fossil fuels to renewable energy sources (RESs) that are ecologically benevolent [2]. Amid the key and most forms of renewable energy, solar power offers a plentiful and permanent way to generate electricity [3]-[5]. Additionally, solar power shows a part in endorsing sustainable development by posing a source of renewable and clean energy [6], [7]. Nevertheless, there are still some difficulties linked with photovoltaic (PV) generation along with its benefits. One of the key troubles is that it is reliant on sunlight that it is a dependable source of energy in regions with restricted sunlight [8].

A DC/DC converter is vital in substantially enhancing PV system's voltage, which includes boost converter that is required in transforming small input DC voltage from low volts to maximum voltage levels [9]. This converter is incorporated into RES to better usage of energy and acts as a foundation for sustainable power generation. Nevertheless, it has maximum ripple current on passive and active components, need a large capacitor value and enormous voltage stress for power switches [10]. A quadratic boost converter is designed in [11] offers maximum voltage gain and improved efficiency. Nevertheless, it has high voltage gains cause significant voltage spikes across switches and other components, necessitating robust design

strategies. The extended single-switch boost converter minimizes the number of components by using only one switch, leading to reduced complexity. While they generally reduce the number of switches, longer duty cycles associated with high voltage gains result in increased losses in the switch and other components [12]. An interleaved Cuk converter is presented in [13] minimize input current ripple by distributing the load current across multiple phases. However, maintaining voltage regulation becomes more complicated with interleaved configurations.

The modified SEPIC converter produce lower input current ripple, enhancing the overall performance and reducing electromagnetic interference (EMI). Nevertheless, it often involves additional components and complexity, which complicate circuit design [14]. To overcome such issues, this research implements a dual stage XBoost converter (DSXBC) in improving PV system's output. Subsequently, maximum power point tracking (MPPT) is implemented in capturing MPP from PV panel [15]. Conventional MPPT approaches comprise perturb and observe (P&O) [16] and incremental conductance (InC) [17] approaches for tracking the upmost power but leads to energy loss and enhanced system expense.

An artificial neural network (ANN)-MPPT has quick convergence speeds and diminished fluctuations nearby the MPP, offering a quicker response to dynamic changes in sunlight. However, its performance is dependent on the specific characteristics of the PV panel being used [18]. The fuzzy based MPPT effectively handle non-linear features of PV systems in variable ecological circumstances, like fluctuations in intensity and temperature. Nevertheless, designing the fuzzy controller requires careful consideration of output and input variables, along with the construction of fuzzy rules [19].

An adaptive network based fuzzy inference system (ANFIS) based MPPT typically exhibits a quicker convergence speed in tracking the MPP. However, ANFIS systems is complex to design and implement due to the need for detailed training and fine-tuning of membership functions [20]. A RNN-MPPT enhance efficiency and adaptation in PV applications, allowing for improved energy output under varying environmental conditions. Nevertheless, introduce latency, particularly in dynamic environments where rapid changes occur [21]. These issues are solved by utilizing radial bias function neural network-MPPT (RBFNN-MPPT) control approach and its parameters are optimized by metaheuristic algorithm, which includes PSO [22], grey wolf optimization (GWO) [23], crow search [24], Harris Hawks optimization (HHO) [25], and firefly optimization (FFO) [26] algorithms. However, that approaches have slow convergence speed, poor performance, difficult design, insufficient exploitation and struggle to detect the global optima.

Research gap: the efficiency and dependability of current PV energy conversion systems are constrained by a number of serious issues. High-gain DC–DC converters frequently suffer from significant voltage spikes, increased switching losses and elevated voltage stress, all of which impair system performance. Conventional MPPT methods, including P&O and InC, simultaneously show slow dynamic response under quickly changing temperature and irradiance circumstances and steady-state oscillations around MPP. Intelligent controllers increase tracking capabilities, but they involve complicated design processes, need a lot of training data and heavily rely on precise parameter tweaking. Furthermore, efficacy of current metaheuristic optimization methods for parameter tweaking is limited in real-time PV applications due to their frequent slow convergence speed, premature convergence and entrapment in local optima.

Consequently, there is a clear research gap in creating an integrated system that concurrently: i) delivers robust global optimization with better convergence, ii) ensures quick and accurate MPPT under dynamic situations, and iii) accomplishes high voltage gain with less stress.

This research proposes a DSXBC combined with a chaotic beetle swarm optimization (CBSO)-optimized RBFNN-based MPPT controller to overcome these difficulties. Through effective global optimization proposed method increases voltage gain, reduces switching stress and improves tracking accuracy.

The primary objectives of proposed research are listed below:

- To design and implement a DSXBC in order to get high voltage gain with less ripple and switching stress.
- To effectively boost low PV output voltage into relatively higher levels, a DSXBC is designed and implemented for attaining high voltage gain with reduced ripple and switching stress.
- To extract maximum power from PV systems, an RBFNN based MPPT controller is integrated which is tuned by CBSO based algorithm for quick tracking in a varying environmental circumstance.

2. PROPOSED METHOD

Figure 1 represents a block diagram indicating a PV based energy conversion system for constant power generation. Initially, the PV system is responsible for transforming irradiation into electrical energy that is characterized by variable output voltage and current that acts as inputs for upcoming stages. Then, the DSXBC is employed in improving PV energy production. It aids to enhance efficacy, mitigate switching losses and sustain reliability of system by regulating voltage stress over semiconductor switches.

Subsequently, PWM generator producing PWM pulses for managing switching function of a DSXBC. These pulses assures the converter functions at optimal duty cycle and switching frequency and dynamically adjust the output voltage and current in changing solar conditions. Conversely, the RBFNN-MPPT controller efficiently tracks the MPP of PV system. Here, the CBSO algorithm tunes the parameter of RBFNN, efficiently sustaining the system at its optimal power generation point. This incorporated approach diminishes losses, improves the performance, sustainability of solar systems and maximizes power extraction.

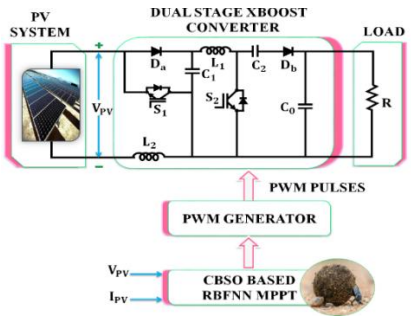

Figure 1. Developed block diagram

2.1. Photovoltaic system

PV is an electrical system that transforms sunlight into power by utilizing panels with the phenomenon of PV effect, the direct electric current is produced from a solar cell, as seen in Figure 2.

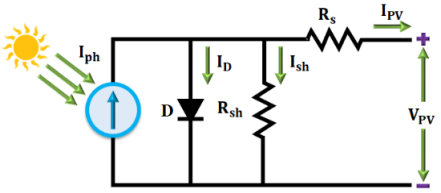

Figure 2. PV system's circuit

For the receiving high power production, the solar cells are joined to form a solar module which is known as solar panel. The PV panel's current on output side as (1) and (2):

$$I_{ph} - I_D - I_{sh} = I_{PV} \quad (1)$$

$$I_{ph} - I_0 \left[exp\left(\frac{V_{PV}+I_{PV}R_S}{N_S v_{tr}}\right) - 1 \right] - \frac{V_{PV}+I_{PV}R_S}{R_{sh}} = I_{PV} \quad (2)$$

Open circuit voltage is computed as (3):

$$V_{OC} = \frac{akT}{q} Log_n \left(\frac{I_{ph}}{I_D} + 1\right) \quad (3)$$

where, series resistance is R_S, shunt resistance is R_{sh}, photo current is I_{ph}, current passing over the shunt resistor is bI_{sh}, ideality constant of diode is a, Boltzmann constant is k, electron's charge is q, number of series connected solar cells is N_s and saturation current of diode is I_D. In this research, the DSXBC is exploited for improving the PV panel's voltage on output side because of its high voltage gain.

2.2. Dual stage XBoost converter

A DSXBC utilizes 2 boost converter phases linked in series to attain a maximum voltage gain. These features make it suitable for various power applications. The circuit of the DSXBC for enhancing the PV system's voltage is represented in Figure 3. Figure 4 represents the waveform of DSXB converter. Figure 5 shows operation Mode 1 and Mode 2 of DSXBC.

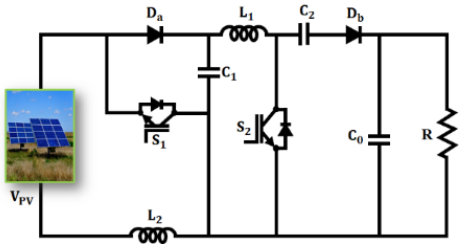

Figure 3. Equivalent circuit of DSXBC

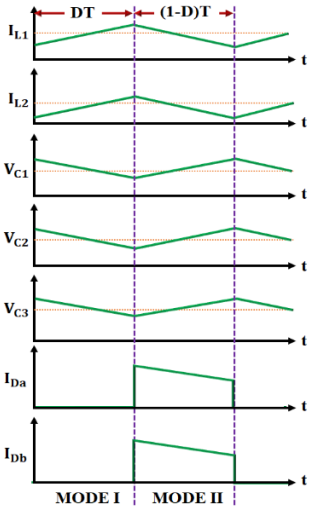

Figure 4. Waveform DSXBC

2.2.1. Mode 1

In this stage, S_1 and S_2 are on and D_b and D_a are inactive, as realized in Figure 5(a). By applying KVL,

$$V_{PV} + V_{C1} = V_{C2} = V_{L1} \quad (4)$$

$$V_{L2} = V_{PV} \quad (5)$$

2.2.2. Mode 2

In this stage, S_1 and S_2 are in inactive condition and D_a and D_b are forward biased and energy stowed in converter's passive components is delivered to the load, as revealed in Figure 5(b). The KVL is applied in stage 2 as (6)-(10):

$$V_{C1} - V_{L1} + V_{C2} - V_O = 0 \quad (6)$$

$$V_O - V_{C1} - V_{C2} = -V_{L1} \quad (7)$$

$$V_O - V_{C1} - (V_{PV} + V_{C1}) = -V_{L1} \quad (8)$$

$$V_{PV} + 2V_{C1} - V_O = V_{L1} \quad (9)$$

$$V_{PV} - V_{C1} = V_{L2} \quad (10)$$

BY utilizing volt-inductor balance,

$$DV_{PV} + (V_{PV} - V_{C1})(1 - D) = 0 \quad (11)$$

$$\frac{V_{PV}}{1-D} = V_{C1} \tag{12}$$

$$(V_{PV} + V_{C1})D + (2V_{C1} + V_{PV} - V_O)(1-D) = 0 \tag{13}$$

$$2V_{C1} - DV_{C1} + V_{PV} - (1-D)V_O = 0 \tag{14}$$

$$V_{C1}(2-D) - (1-D)V_O + V_{PV} = 0 \tag{15}$$

$$-(1-D)V_O + \frac{(2-D)V_{PV}}{(1-D)} + V_{PV} = 0 \tag{16}$$

$$V_O(1-D) = \frac{2V_{PV} - V_{PV}D + V_{PV} - V_{PV}D}{(1-D)} \tag{17}$$

$$(1-D)V_O = \frac{3V_{PV} - 2V_{PV}D}{1-D} \tag{18}$$

$$\frac{V_O}{V_{PV}} = \frac{(3-2D)}{(1-D)^2} \tag{19}$$

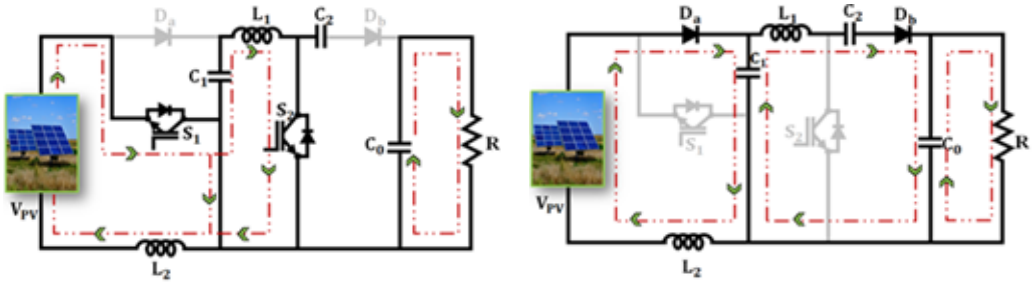

(a) (b)

Figure 5. Operation for; (a) Mode 1 and (b) Mode 2 of DSXBC

2.2.3. Designing of inductance value

The objective of designing an inductor is to function the converter in CCM:

$$V_{PV} + V_{C1} = L_1 \frac{dI_{L1}}{dt} = \frac{V_{PV} - V_{PV}D + V_{PV}}{1-D} \tag{20}$$

$$L_1 \frac{\Delta I_{L1}}{dt} = \frac{2V_{PV} - V_{PV}D}{1-D} \tag{21}$$

$$\frac{V_O}{R} L_1 \geq \frac{V_{PV}(2-D)DT}{2} \tag{22}$$

$$V_O L_1 \geq \frac{RV_{PV}(2-D)DT}{2} \tag{23}$$

$$L_1 \geq \frac{R(1-D)^2(2-D)D}{2(3-2D)f_s} \tag{24}$$

where, the duty ratio is indicated by D, load is R and desirable inductance is L and switching frequency is f_s. The voltage across L_1, L_2, C_1, and C_2 are signified as V_{L1}, V_{L2}, V_{C1}, $and\ V_{C2}$. For inductor L_2,

$$L_2 \geq \frac{R(1-D)^4D^2}{2f_s(3-2D)(1+D-D^2)} \tag{25}$$

2.2.4. Designing of capacitance value

The selection of a capacitor is based on a highest permissible voltage ripple and a voltage across the capacitor.

$$I_{C1}\Delta T = C_1\Delta V_{C1} \quad (26)$$

$$I_{C1}DT = \Delta V_{C1}C_1 \quad (27)$$

$$\frac{V_O}{R(1-D)} = \Delta V_{C1}C_1 \quad (28)$$

$$\frac{V_O}{R(1-D)f_S\Delta V_{C1}} = C_1 \quad (29)$$

$$\frac{V_{PV}(3-2D)}{(1-D)^2R(1-D)f_S\Delta V_{C1}} = V_{C1} \quad (30)$$

$$\frac{V_{PV}(3-2D)}{R(1-D)^3f_S\Delta V_{C1}} = C_1 \quad (31)$$

For C_2 and C_3,

$$\frac{V_{PV}(3-2D)}{R(1-D)^2f_S\Delta V_{C2}} = C_2 \quad (32)$$

$$\frac{V_{PV}(3-2D)}{R(1-D)^2f_S\Delta V_{C3}} = C_3 \quad (33)$$

where, the required capacitance is represented by C, input voltage is V_{PV} and allowable ripple in the voltage of capacitor is ΔV_C. Thus, the converter offers better solution for overcoming environmental changes and enhances the efficacy. Then, the highest power is tracked by RBFNN-MPPT controller and is performance is enhanced by the CBSO algorithm.

2.3. Chaotic beetle swarm optimization based RBFNN-MPPT

In the developed research, the parameters of a RBFNN-MPPT is tracks PV system's uppermost power. Structure of RBFNN-MPPT comprises input, output and a hidden layer to maintain data processing tasks.

$$net_j^1 = x_i^1 \quad (34)$$

$$y_{1\,j}^1 = f^1\left(net_j^1\right) = (x_i^1)\ where\ j = 1,.n; i = 1,2. \quad (35)$$

whereas, x_i^1 indicates the input layer, $f^1\left(net_j^1\right)$ indicates the net total of nodes that is provided to the hidden layer. The hidden layer that utilizes Gaussian functions. This layer has a large number of neurons. Selecting neurons for this layer is a difficult process. Thus, it proposed a way to select neurons for the hidden layer while maintaining the data structure. Each neuron in the hidden layer has an RBF that is centered at a point based on complexity of the input and output variables. The fundamental functions, which rely on the variables $\left\{w_{1\,j}^1, b_j^1\right\}$ and input activations x_j^1, detect the hidden unit activations. Each dimension has a distinct radius for the RBF function. During the training phase, thespreads and centers of network are selected. Both the net input and output are:

$$net_j^1 = \sum_j w_{1\,j}^1\, y_{1\,j}^1 \quad (36)$$

$$y_{1\,j}^2 = f^2\left(w_{1\,j}^1 y_{1\,j}^1 + b_j^1\right) where\ j = 1 \cdots n \quad (37)$$

The hidden layer's bias terms are represented by $b_j^1$and the weights that link to the input and hidden layers are specified by $w_{1\,j}^1$. The Gaussian function's outputs are joined in the linear layer. In training, the weights among the output and hidden layers are changed and computed. The input and output of overall RBFNN is,

$$\frac{d\omega_r}{dt} = b + \sum_{j=1}^{n} v_j exp\left(-\frac{\|x-c_j\|^2}{\beta^2 j}\right) \quad (38)$$

where, the number of RBF units is indicated by n, weight and bias term are v_j and b. However, tuning method is required to attain high PV power. Therefore, the CBSO algorithm is exploited in this research, which enhances the beetle swarm optimization (BSO) algorithm by introducing chaotic sequences, preventing premature convergence and enhancing global optimization capability.

In the beginning, the parameters of RBFNN comprising biases, weights, centers and spreads of Gaussian activation functions are randomly initialized. Then, the chaotic sequences are exploited to set initial positions of beetles in the solution space. The position of each beetle X_i indicates a potential solution for parameters of RBFNN-MPPT. Then, the chaotic mapping incorporates chaotic sequences that are inherently random yet deterministic, offering an efficiency way to diversify the initial population. This averts beetles from premature clustering, improving search efficacy. The logistic chaotic map is commonly exploited that is defined by (39):

$$z_{k+1} = \mu z_k(1 - z_k), z_k \in (0,1), \mu\ [3.57,4] \tag{39}$$

where, chaotic variable at iteration k is z_k, μ manages the chaotic dynamics. By exploiting this chaotic sequence, X_i is initialized, offering high diversity and coverage of the search space. Each beetle's position is updated according to the fitness value at the position of antennae. It incorporates beetle sensory information and velocity, as (40):

$$X_{is}^{k+1} = X_{is}^{k} + \lambda V_{is}^{k} + (1 - \lambda)\xi_{is}^{k} \tag{40}$$

where, speed of beetles is V_{is}, increase in movement of beetle position is ξ_{is}, positive constant is $\lambda, s = 1,2,\cdots,S; i = 1,2,\cdots,n$. The speed is updated by (41):

$$\omega V_{is}^{k} + \left(P_{is}^{k} - X_{is}^{k}\right)c_1 r_1 + \left(P_{gs}^{k} - X_{gs}^{k}\right)c_2 r_2 = V_{is}^{k+1} \tag{41}$$

where, random functions in the range $[0,1]$ is r_1 and r_2, 2 positive constants are $c_1$and c_2, inertia weight is ω and is fixed constant. The decreasing inertia weight is (42):

$$\omega = \omega_{max} - \frac{\omega_{max} - \omega_{min}}{K} * k \tag{42}$$

where, current and maximum number of iterations are denoted by $k\ and\ K$, maximum and minimum value of ω is ω_{max} and ω_{min}. The ξ function is (43):

$$\xi_{is}^{k+1} = \delta^k * V_{is}^{k} * sign\left(\left(f(X_{rs}^{k}) - f(X_{rs}^{k})\right)\right) \tag{43}$$

where, the fitness function estimating the MPP is $f(.)$ and adaptive step size is δ^k. In the Beetle antennae searching phase, each beetle explores the solution space by exploiting the sensory principle of beetle antennae search. 2 antennae positions are produced around the current position of beetle to probe the local gradient in parameter space. For beetle i, the antennae positions at iteration t are,

$$X_{rs}^{k+1} = X_{rs}^{k} + \frac{d}{2}V_{is}^{k} \tag{44}$$

$$X_{ls}^{k+1} = X_{ls}^{k} - \frac{d}{2}V_{is}^{k} \tag{45}$$

where, random direction vector is denoted by V_{is}^{k}, sensing length among antennae is d and left and right antennae positions are X_{ls}^{k} and X_{rs}^{k}. For the current position of beetle, the fitness evaluation is performed to improve the parameters of RBFNN-MPPT. The iteration count is 100 when the population size is 50. Figure 6 displays the flowchart of CBSO based RBFNN-MPPT controller. Then, the chaotic sequence is continually applied at each iteration to adjust beetle positions and step size adaptively, assuring sustained diversity. To sssure refined local search, the step size δ^k and antennae distance is adjusted dynamically as (46) and (47):

$$\delta^{k+1} = \eta\delta^k \tag{46}$$

$$d^{k+1} = c_2\delta^k \tag{47}$$

where, the convergence speed is managed by η. The optimal beetle positions corresponds to the optimized set of RBFNN parameters at the end of CBSO. These parameters results in maximum PV power extraction with improved tracking efficacy and diminished steady state oscillations. The developed controller improves the dynamic performance of PV system by efficiently managing fluctuations in solar temperature and irradiance, demonstrates the enhancements in adaptability and robustness.

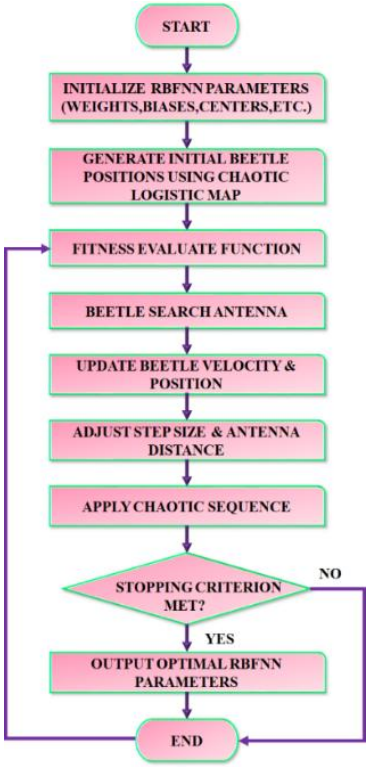

Figure 6. Flowchart of CBSO based RBFNN-MPPT controller

3. RESULT AND DISCUSSIONS

This part analyzes an outcome of DSXBC with CBSO based RBFNN-MPPT controller. The parameters for developed work with solver details is denoted in Table 1. The research is applied in MATLAB tool and investigation with conventional approaches are included in this section.

Table 1. Parameters for developed research

Parameter		Specification	
PV system		Solver details	
Cell linked in series	36	Type	Variable step
Voltage(open circuit)	37.25 V	Solver	ode 45
Rated power	10000 W	Min. step size	auto
Panels in series	4	Relative tolerance	1e-3
Panels in parallel	11	Max. step size	1e-6
Current(short circuit)	8.95 A	Initial step size/absolute tolerance	auto
		DSXBC	
C_1, C_2	22 µF	Switching frequency	10 KHz
L_1, L_2	4.7 mH	C_O	2200 µF

The behaviour of PV system in steady state condition is represented in Figure 7. The temperature is settled at 32 ℃ with no oscillations while irradiance maintained at 950 $(W/Sq.m)$. Consequently, voltage is continued at 110 V in whole system and current on input side is progressively decreased and stabilized at 35 V with little variations. These current and voltage are effectively raised by a DSXBC.

Figure 8 illustrates an output waveform of DSXBC. The output voltage has small value in the beginning and CBSO based RBFNN MPPT controller tracks the maximum power and raised to 320 V throughout the system. Also, a current on output side is progressively elevated and continued at 12 A with no more fluctuations. Input power is increased in an initial stage and stabilized at 3600 W in the entire system. Furthermore, an output power is dropped sharply and then stabilized at 3800 W without oscillations.

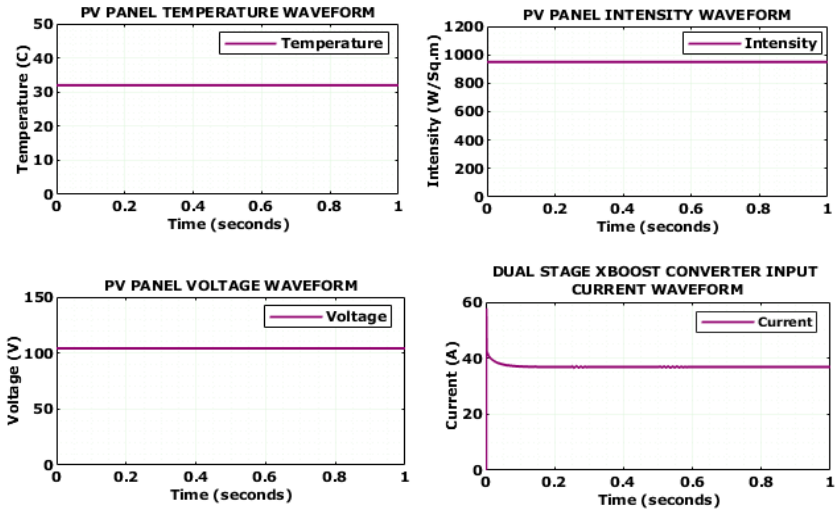

Figure 7. PV system's behaviour in steady state scenario

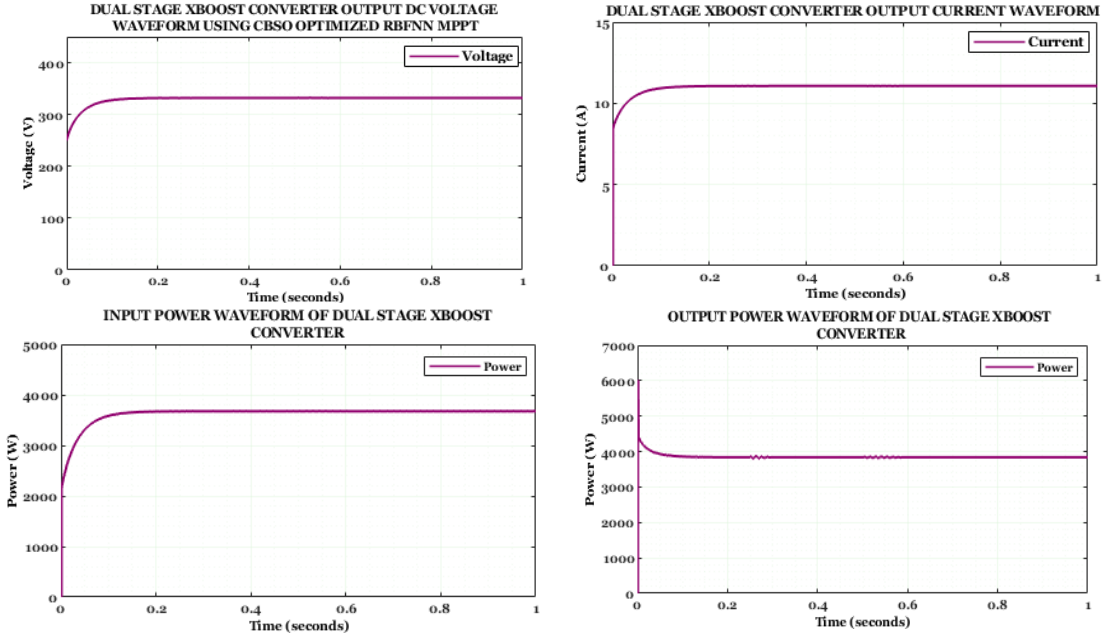

Figure 8. Output waveform of DSXBC

The waveform of PV system in changing condition is displayed in Figure 9. The temperature is initially changed in the starting stage and stabilized at 32 ℃ and an irradiance is continued at 950 $(W/Sq.m)$ in complete system. Then, voltage of PV is randomly changed due to the changes in temperature and intensity and then, it is maintained at 110 V. Moreover, an input current is gradually elevated and stabilized at 50 A with slight alterations.

Figure 10 presents an output waveform of DSXBC. The output voltage is arbitrarily altered in the initial stage and maintained at 380 V while an output current settled at 12.5 A all over the system. An input power is slowly elevated and maintained at 4900 W while an output power has initial variations and continued at 5100 W with less alternations.

The behaviour of PV system is revealed in Figure 11. Initially, the temperature has small value and sustained at 32 ℃ whereas, the intensity is continued at 950 $(W/Sq.m)$. Later, the voltage is slowly improved and stabilized at 110 V and input current has the value of 35 A with few more fluctuations.

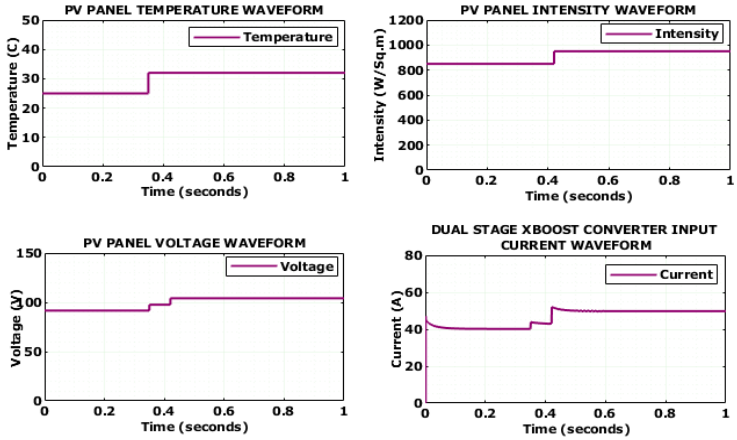

Figure 9. Waveform of PV system in changing circumstance

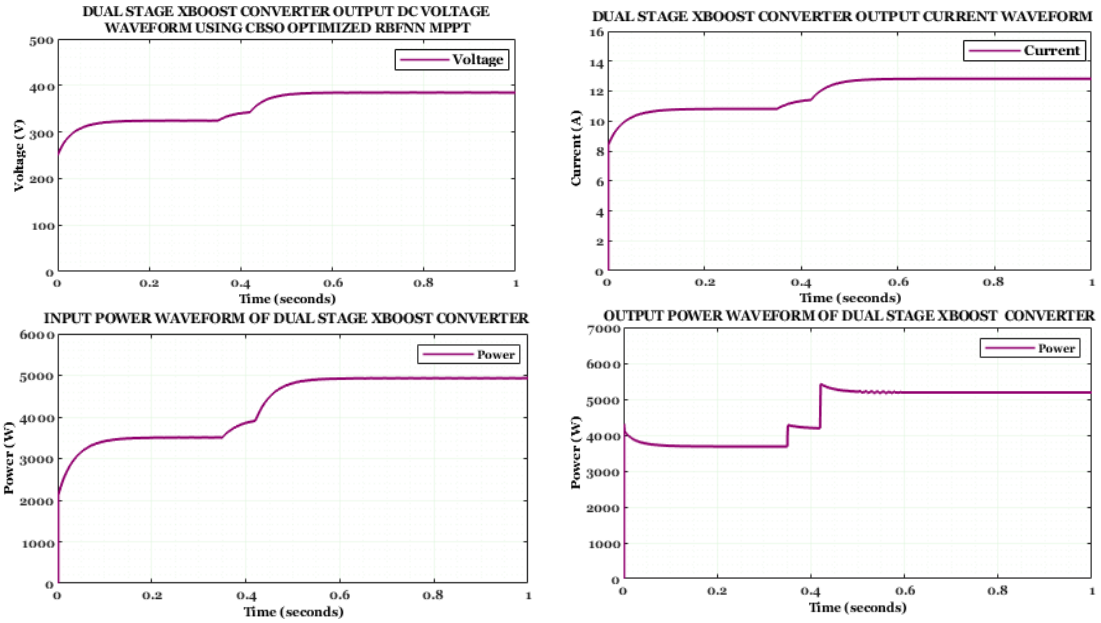

Figure 10. Output waveform of DSXBC

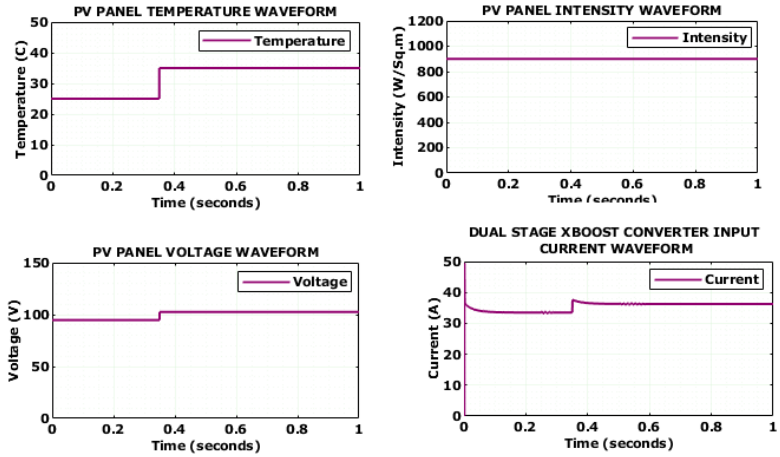

Figure 11. Characteristics of PV system in constant irradiation and varying temperature scenario

An output of DSXBC is showed in Figure 12. Output voltage is gradually raised and continued at 320 V in entire system. Consequently, current increased initially and stabilized at 12 A with no more oscillations. Input power is leisurely altered and sustained at 3500 W whereas an output power is maintained a stable value at 3700 W in the entire system.

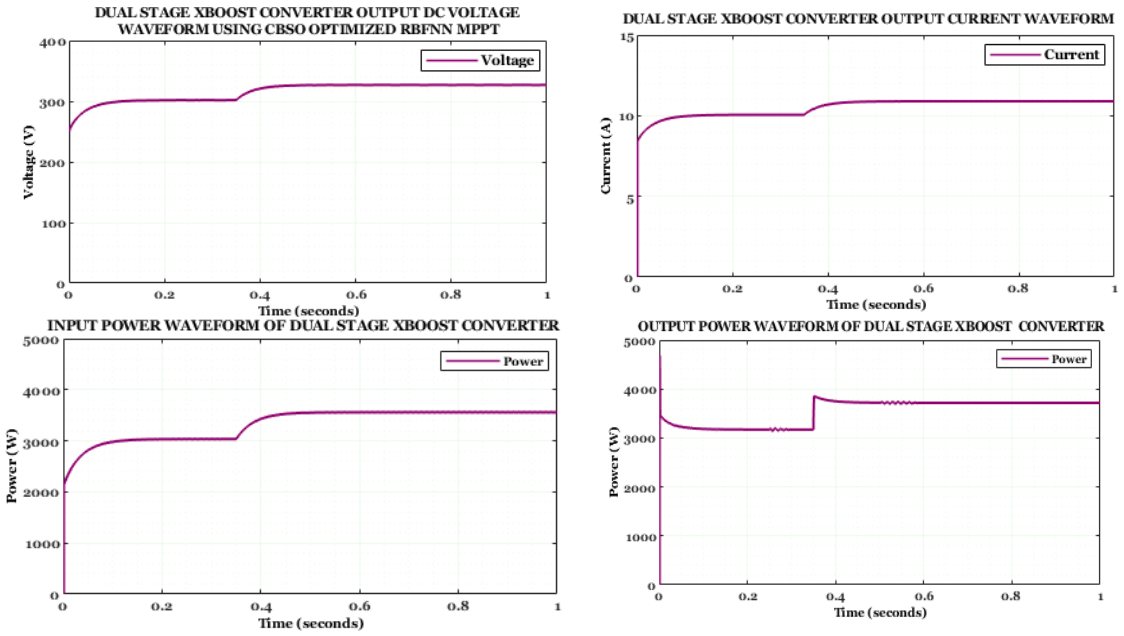

Figure 12. Output waveform of DSXBC

Figure 13 displays the comparison of efficiency for interleaved boost converter (IBC) [27], coupled inductor IBC [28], transformer less step-up [29], step-up/down [30], and developed approach that attains highest efficacy of 99.74% than other approaches, indicating the superior performance of DSXBC. It validates the efficacy of the developed approach in improving power conversion efficacy and reducing losses.

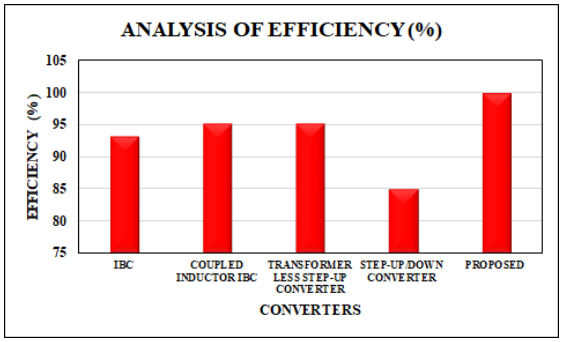

Figure 13. Comparison of efficiency among converters

An analysis of voltage gain for Quadratic boost [31], Quasi Z source [32], and DSXBC is represented in Figure 14(a). The maximum voltage gain is attained by DSXBC compared to other approaches. It highlights the better step-up ability of DSXBC in high duty cycle, making it more efficient in high voltage applications. Figure 14(b) illustrates voltage stress for non-isolated [33], quadratic boost [34], non-isolated quadratic boost [35], and DSXBC, which has less voltage stress on switch than other approaches. It validates the developed approach has diminished switching stress, thereby improving efficacy and reliability of power system.

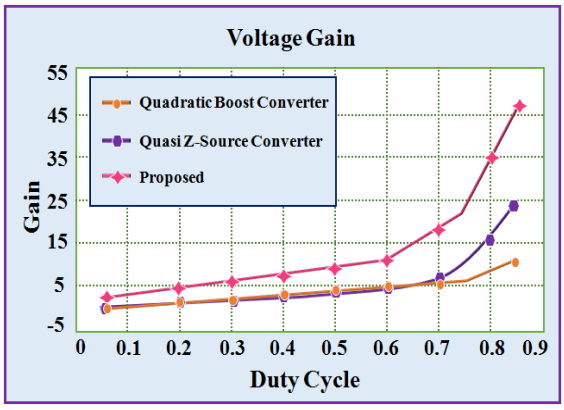

(a)

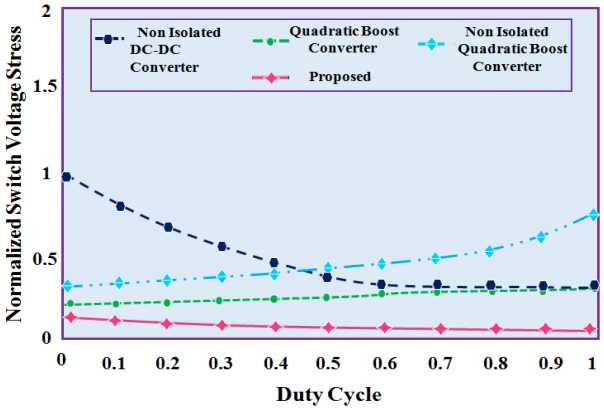

(b)

Figure 14. Comparison of converters; (a) voltage gain and (b) voltage stress

An analysis of tracking efficiency for P&O, ANN, fuzzy SMC [36], MPC [37], and CBSO-RBFNN MPPT approach is shown in Figure 15. The CBSO-RBFNN MPPT attains the better tracking efficiency of 98.9%, there by attaining more and faster accurate tracking in changing operating conditions.

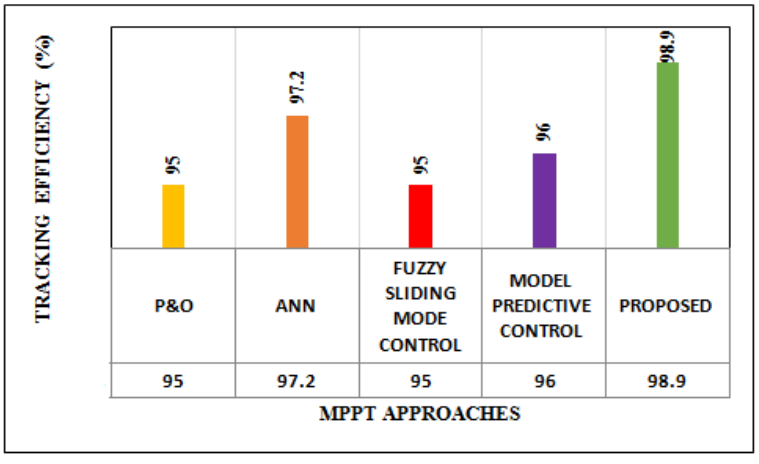

Figure 15. Analysis of tracking efficiency for MPPT approaches

4. CONCLUSION

This research proposed a DSXBC integrated with a CBSO-based RBFNN-MPPT controller for generating solar power efficiently and steadily. By lowering voltage stress and switching ripple and greatly

increasing voltage gain, DSXBC increased power conversion stage's dependability. Consistent maximum power extraction under various operating situations is made possible by CBSO-optimized RBFNN controller, which ensures quick convergence and reduced steady-state oscillations.

The following is a summary of the main numerical contributions of proposed system: i) proposed converter attained 99.74% energy conversion efficiency with improved voltage gain, surpassing that of traditional converters and ii) CBSO-based RBFNN-MPPT controller achieved 98.9% tracking efficiency, which is better than P&O and ANN-based methods.

Even with these advancements, there are still certain limitations. Only MATLAB/Simulink simulations are used to validate proposed system, hardware implementation is not used. Furthermore, sensor noise, sudden environmental disruptions and partial shading are not taken into account when evaluating the performance. Additionally, there is no experimental validation of the CBSO-RBFNN controller's computational complexity and real-time viability.

Future research will concentrate on: i) implementing proposed system into practice for hardware certification on real-time embedded platforms, ii) assessing performance in situations with non-uniform irradiance and partial shade, iii) examining controller complexity and real-time computational efficiency, and iv) expanding the strategy to include hybrid and grid-connected renewable energy systems.

FUNDING INFORMATION

Authors state no funding involved.

AUTHOR CONTRIBUTIONS STATEMENT

This journal uses the Contributor Roles Taxonomy (CRediT) to recognize individual author contributions, reduce authorship disputes, and facilitate collaboration.

Name of Author	C	M	So	Va	Fo	I	R	D	O	E	Vi	Su	P	Fu
Sreenivasan Ramachandran	✓	✓			✓	✓		✓	✓	✓				
Ramkumar Ravindran		✓		✓	✓					✓	✓	✓	✓	

C : **C**onceptualization
M : **M**ethodology
So : **So**ftware
Va : **Va**lidation
Fo : **Fo**rmal analysis
I : **I**nvestigation
R : **R**esources
D : **D**ata Curation
O : Writing -**O**riginal Draft
E : Writing - Review &**E**diting
Vi : **Vi**sualization
Su : **Su**pervision
P : **P**roject administration
Fu : **Fu**nding acquisition

CONFLICT OF INTEREST STATEMENT

Authors have no conflicts of interest relevant to this article to declare.

DATA AVAILABILITY

Data are available from the author upon reasonable request.

REFERENCES

[1] M. T. Hussain *et al.*, "Enhanced MPP Tracking in Partial Shading Conditions for Solar PV Systems: A Metaheuristic Approach Utilizing Projectile Search Algorithm," *IEEE Access*, vol. 13, pp. 50895–50917, 2025, doi: 10.1109/ACCESS.2025.3546351.

[2] N. A. Kadhim, A. A. Obed, A. J. Abid, H. Kotb, and A. Emara, "Optimal PV Reconfiguration Under Partial Shading Based on White Shark Optimization," *IEEE Access*, vol. 12, pp. 27385–27398, 2024, doi: 10.1109/ACCESS.2024.3367833.

[3] M. Abdelsattar, M. A. Ismeil, M. M. AZayed, A. Abdelmoety, and A. Emad-Eldeen, "Assessing Machine Learning Approaches for Photovoltaic Energy Prediction in Sustainable Energy Systems," *IEEE Access*, vol. 12, pp. 107599–107615, 2024, doi: 10.1109/ACCESS.2024.3437191.

[4] I. Hassan *et al.*, "Explainable Deep Learning Model for Grid-Connected Photovoltaic System Performance Assessment for Improving System Reliability," *IEEE Access*, vol. 12, pp. 120729–120746, 2024, doi: 10.1109/ACCESS.2024.3452778.

[5] A. Saxena *et al.*, "Intelligent load forecasting and renewable energy integration for enhanced grid reliability," *IEEE Transactions on Industry Applications*, vol. 60, no. 6, pp. 8403–8417, 2024, doi: 10.1109/TIA.2024.3436471.

[6] B. Modu, M. P. B. Abdullah, A. Alkassem, H. Z. Al Garni, and M. Alkabi, "Optimal design of a grid-independent solar-fuel cell-biomass energy system using an enhanced salp swarm algorithm considering rule-based energy management strategy," *IEEE Access*, vol. 12, pp. 23914–23929, 2024, doi: 10.1109/ACCESS.2024.3362241.

[7] K. S. Kavin, P. S. Karuvelam, M. D. Raj, and M. Sivasubramanian, "A Novel KSK Converter with Machine Learning MPPT for PV Applications," *Electric Power Components and Systems*, pp. 1–19, 2024, doi: 10.1080/15325008.2024.2346806.
[8] O. Abdel-Rahim, M. L. Alghaythi, M. S. Alshammari, and D. S. Osheba, "Enhancing Photovoltaic Conversion Efficiency With Model Predictive Control-Based Sensor-Reduced Maximum Power Point Tracking in Modified SEPIC Converters," *IEEE Access*, vol. 11, pp. 100769–100780, 2023, doi: 10.1109/ACCESS.2023.3315150.
[9] C. H. Lin, M. S. Khan, J. Ahmad, H. D. Liu, and T. C. Hsiao, "Design and Analysis of Novel High-Gain Boost Converter for Renewable Energy Systems (RES)," *IEEE Access*, vol. 12, pp. 24262–24273, 2024, doi: 10.1109/ACCESS.2024.3365705.
[10] A. Raj, and R. P. Praveen, "Highly efficient DC-DC boost converter implemented with improved MPPT algorithm for utility level photovoltaic applications," *Ain Shams Engineering Journal*, vol. 13, no. 3, pp. 101617, 2022, doi: 10.1016/j.asej.2021.10.012.
[11] F. Alonge, F. D'ippolito, G. Garraffa, G. C. Giaconia, R. Latona, and A. Sferlazza, "Sliding mode control of quadratic boost converters based on min-type control strategy," *IEEE Access*, vol. 11, pp. 39176–39184, 2023, doi: 10.1109/ACCESS.2023.3267984.
[12] A. S. Mansour, and M. S. Zaky, "A new extended single-switch high gain DC–DC boost converter for renewable energy applications," *Scientific Reports*, vol. 13, no. 1, pp. 264, 2023, doi: 10.1038/s41598-022-26660-7.
[13] N. T. Kalantari, S. G. Sani, and Y. Sarsabahi, "Implementation and design of an interleaved Cuk converter with selective input current ripple elimination capability," *International Journal of Circuit Theory and Applications*, vol. 49, no. 6, pp. 1743–1756, 2021, doi: 10.1002/cta.2940.
[14] J. Kathiresan, S. K. Natarajan, and G. Jothimani, "Design and implementation of modified SEPIC high gain DC-DC converter for DC microgrid applications," *International Transactions on Electrical Energy Systems*, vol. 31, no. 8, pp. e12921, 2021, doi: 10.1002/2050-7038.12921.
[15] K. S. Kavin, P. S. Karuvelam, M. Matcha, and S. Vendoti, "Improved BRBFNN-based MPPT algorithm for coupled inductor KSK converter for sustainable PV system applications," *Electrical Engineering*, pp. 1–23, 2025, doi: 10.1007/s00202-025-02952-9.
[16] M. Sedraoui *et al.*, "Development of a fixed-order controller for a robust P&O-MPPT strategy to control poly-crystalline solar PV energy systems," *Scientific reports*, vol. 15, no. 1, pp. 2923, 2025, doi: 10.1038/s41598-025-86477-y.
[17] M. A. B. Siddique, A. Asad, R. M. Asif, A. U. Rehman, M. T. Sadiq, and I. Ullah, "Implementation of incremental conductance MPPT algorithm with integral regulator by using boost converter in grid-connected PV array," *IETE Journal of Research*, vol. 69, no. 6, pp. 3822–3835, 2023, doi: 10.1080/03772063.2021.1920481.
[18] N. F. Ibrahim *et al.*, "Operation of grid-connected PV system with ANN-based MPPT and an optimized LCL filter using GRG algorithm for enhanced power quality," *IEEE Access*, vol. 11, pp. 106859–106876, 2023, doi: 10.1109/ACCESS.2023.3317980.
[19] K. Ullah, M. Ishaq, F. Tchier, H. Ahmad, and Z. Ahmad, "Fuzzy-based maximum power point tracking (MPPT) control system for photovoltaic power generation system," *Results in Engineering*, vol. 20, pp. 101466, 2023, doi: 10.1016/j.rineng.2023.101466.
[20] S. R. Revathy *et al.*, "Design and analysis of ANFIS–based MPPT method for solar photovoltaic applications," *International Journal of Photoenergy*, vol. 2022, no. 1, pp. 9625564, 2022, doi: 10.1155/2022/9625564.
[21] C. Jiang, "African vulture optimized RNN algorithm maximum power point tracking (MPPT) controller for photovoltaic (PV) system," *Measurement: Sensors*, vol. 36, pp. 101392, 2024, doi: 10.1016/j.measen.2024.101392.
[22] A. del Rio, O. Barambones, J. Uralde, E. Artetxe, and I. Calvo, "Particle swarm optimization-based control for maximum power point tracking implemented in a real time photovoltaic system," *Information*, vol. 14, no. 10, pp. 556, 2023, doi: 10.3390/info14100556.
[23] S. Motahhir, S. Chtita, A. Chouder, and A. EI Hammoumi, "Enhanced energy output from a PV system under partial shaded conditions through grey wolf optimizer," *Cleaner Engineering and Technology*, vol. 9, pp. 100533, 2022, doi: 10.1016/j.clet.2022.100533.
[24] M. Ben Smida, A. T. Azar, A. Sakly, and I. A. Hameed, "Analyzing grid connected shaded photovoltaic systems with steady state stability and crow search MPPT control," *Frontiers in Energy Research*, vol. 12, pp. 1381376, 2024, doi: 10.3389/fenrg.2024.1381376.
[25] X. Tao *et al.*, "A Novel Harris-Hawk-Optimization-Based Maximum-Power-Point-Tracking Control Strategy for a Grid-Connected PV Power-Generation System," *Energies*, vol. 17, no. 1, pp.76, 2023, doi: 10.3390/en17010076.
[26] R. B. Watanabe *et al.*, "Implementation of the bio-inspired metaheuristic firefly algorithm (FA) applied to maximum power point tracking of photovoltaic systems," *Energies*, vol. 15, no. 15, pp. 5338, 2022, doi: 10.3390/en15155338.
[27] A. A. Al-Samawi, A. S. Atiyah, and A. H. Al-Jrew, "Power Optimization of Partially Shaded PV System Using Interleaved Boost Converter-Based Fuzzy Logic Method," *Eng*, vol. 6, no. 8, pp. 201, 2025, doi: 10.3390/eng6080201.
[28] K. S. Kavin, P. S. Karuvelam, N. Kumar, S. Kar, R. A. Rahiman, and S. Patwa, "Coupled inductor interleaved boost converter with ANN and RNN based MPPT algorithm for PV system," *International Journal of Applied Power Engineering (IJAPE)*, vol. 13, no. 3, 2024, doi: 10.11591/ijape.v13.i3.pp616-627.
[29] A. Imanlou, R. Behkam, A. Nadermohammadi, and H. Nafisi, "A New High Voltage Gain Transformer-Less Step-Up DC-DC Converter with Double Duty-Cycles: Design and Analysis," *IEEE Access*, 2024, doi: 10.1109/ACCESS.2024.3425724.
[30] N. Yadav *et al.*, "Performance evaluation of step-up/down partial power converters based on current-fed DC-DC topologies," *IEEE Transactions on Industry Applications*, vol. 60, no. 5, pp. 7111-7124, 2024, doi: 10.1109/TIA.2024.3413050.
[31] G. Li, X. Jin, X. Chen, and X. Mu, "A novel quadratic boost converter with low inductor currents," *CPSS Transactions on Power Electronics and Applications*, vol.5, no. 1, pp. 1–10, 2020, doi: 10.24295/CPSSTPEA.2020.00001.
[32] P. Padmavathi and S. Natarajan, "Single switch quasi Z-source based high voltage gain DC-DC converter," *International Transactions on Electrical Energy Systems*, vol. 30, p. e12399, 2020, doi: 10.1002/2050-7038.12399.
[33] R. Rajesh, N. Prabaharan, and T. K. Santhosh, "Design and analysis of a non-isolated DC-DC converter with a high-voltage conversion ratio," *IEEE Transactions on Circuits and Systems II: Express Briefs*, vol. 70, no. 6, pp. 2036–2041, 2023, doi: 10.1109/TCSII.2022.3226187.
[34] S. Hasanpour, Y. Siwakoti, and F. Blaabjerg, "New Single-Switch quadratic boost DC/DC converter with low voltage stress for renewable energy applications," *IET Power Electron*, vol. 13, no. 19, pp. 4592–4600, 2020, doi: 10.1049/iet-pel.2020.0580.
[35] M. Izadi, A. Mosallanejad, and A. L. Eshkevari, "A non-isolated quadratic boost converter with improved gain, high efficiency, and continuous input current," *IET Power Electron*, vol. 16, no. 2, pp. 193–208, 2023, doi: 10.1049/pel2.12376.
[36] M. S. Adouairi, B. Bossoufi, S. Motahhir, and I. Saady, "Application of fuzzy sliding mode control on a single-stage grid-connected PV system based on the voltage-oriented control strategy," *Results in Engineering*, vol. 17, pp. 100822, 2023, doi: 10.1016/j.rineng.2022.100822.
[37] Y. Zhao, A. An, Y. Xu, Q. Wang, and M. Wang, "Model predictive control of grid-connected PV power generation system considering optimal MPPT control of PV modules," *Protection and Control of Modern Power Systems*, vol. 6, pp. 1–12, 2021, doi: 10.1186/s41601-021-00210-1.

BIOGRAPHIES OF AUTHORS

Sreenivasan Ramachandran is currently doing as a Research Scholar in the Department of Electrical and Electronics Engineering at Dhanalakshmi Srinivasan University, School of Engineering and Technology, Samayapuram, Trichy-621112, India. He completed his M.E. in Thangavelu Engineering College, Chennai (2014). He completed his B.E. in Thangavelu Engineering College, Chennai (2010). He can be contacted at email: srini.vasan256@gmail.com.

Ramkumar Ravindran is currently working as an Associate professor in the Department of Electrical and Electronics Engineering at Dhanalakshmi Srinivasan University, Trichy. He obtained his Ph.D. under Faculty of Electrical Engineering from Anna University (2022), Chennai. He completed his M.E in Sethu Institute of Technology (2012), Madurai. He completed his B.E. in K.L.N. College of Information Technology (2008), Madurai. He has published more than 38 Scopus indexed journals and 6 SCI journals in his field. He has published 22 patents and 3 grant patents in his field. He has presented papers in 28 International conferences. He has 11 years of teaching experience and 1-year industrial experience. His area of interest is power electronic converters, renewable energy, and micro grid. He can be contacted at email: 2019ramkr@gmail.com.